

## NEUTRON SCATTERING ON DEFORMED NUCLEI\*

L. F. Hansen, R. C. Haight, B. A. Pöhl, C. Wong  
Lawrence Livermore National Laboratory, Livermore, CA 94550

Ch. Lagrange  
Centre d'Etudes de Bruyeres-le-Chatel, France.

### ABSTRACT

Measurements of neutron elastic and inelastic differential cross sections around 14 MeV for  $^9\text{Be}$ , C,  $^{181}\text{Ta}$ ,  $^{232}\text{Th}$ ,  $^{238}\text{U}$ , and  $^{239}\text{Pu}$  have been analyzed using a coupled channel (CC) formalism for deformed nuclei and phenomenological global optical model potentials (OMP). For the actinide targets these results are compared with the predictions of a semi-microscopic calculation using Jeukenne, Lejeune, and Mahaux (JLM) microscopic OMP and a deformed ground state nuclear density. The overall agreement between calculations and the measurements is reasonable good even for the very light nuclei, where the quality of the fits is better than those obtained with spherical OMP.

### EXPERIMENTAL RESULTS AND CALCULATIONS

The elastic differential cross sections from Be, C, and Ta measured at 14.6 MeV (Fig. 1), and those from Th, U, and Pu, measured at 14.1 MeV (Fig. 4), were reported earlier.<sup>1</sup> New measurements were carried out for the differential elastic and inelastic (4.43 MeV level) cross sections from carbon for 13.6, 13.85, 14.04, 14.35, 14.66, and 14.80 MeV neutrons (Figs. 2,3). The relatively small energy spacings at which the data were taken were intended 1) to look for changes in the shape of the angular distributions around 14 MeV as suggested by resonance structure in the C total cross section; and 2) by subtraction to look for structure in the (n, $\alpha$ ) cross section in this energy range.

The nuclei discussed in the present work are all characterized by large quadrupole deformations,  $0.2 < \beta_2 \leq 1.2$ . This suggests the need for deformed OMP when calculating the differential scattering cross sections to account for the strong couplings between the ground state (GS) and the low excited levels of the GS rotational band. The CC calculations have been performed with the code ECIS79 starting with phenomenological potentials with global OMP parameters optimized to fit neutron data.<sup>2-4</sup> For  $^9\text{Be}$  and C, CC calculations were carried out with two OMP: a) the spherical potential of Ref. 2, by reducing the imaginary potential,  $W_D$ , by 25% to correct for coupling effects.<sup>5</sup> The fits to the data were obtained by a least squares analysis of the strengths of  $V_R$  and  $W_D$ . After search, the fits to the measured angular distributions were indistinguishable from those obtained with the spherical potential (Fig. 1, dashed lines) and consequently they have not been plotted. b) A second CC calculation was carried out to fit the elastic and inelastic (4.43 MeV) angular distributions

for C between 13.60-14.80 MeV, using the deformed OMP given by Meigooni et. al.<sup>3</sup> This latter potential was obtained from fitting neutron scattering from C over a wide energy range. The CC calculations with this potential (discussed below), have given a much better fit to the data.

${}^9\text{Be}(n,n_0)$ . The CC calculations include the GS (3/2-), the 2.429 (5/2-), and 6.660 (7/2-) excited levels. The value of  $\beta_2$  is 1.2 and the Legendre multipole expansion of  $V_R$  and  $W_D$  include terms up to  $\ell = 6$  for all the calculations. The best fit to the Be cross sections, Fig. 1 (solid line) was calculated with the deformed OMP that gave the best fit to the C data (Table 1-SetB).

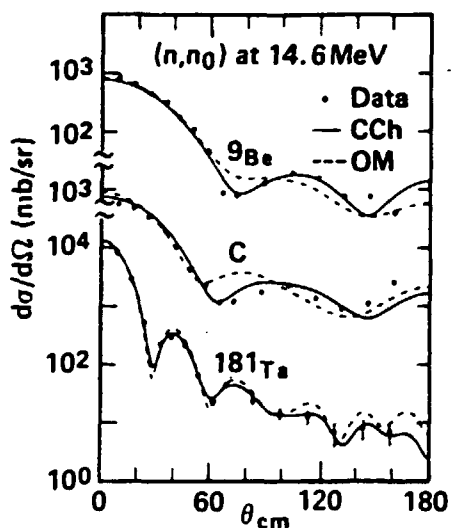


Figure 1

C(n,n<sub>0</sub>) and C(n,n'). The measured angular distributions for the elastic and inelastic (4.43 MeV) at 13.60, 13.85, 14.04, 14.66, and 14.80 MeV are shown in Figs. 2 and 3 respectively. The data are in good agreement with measurements found in the literature<sup>6,7</sup> for some of these energies. Furthermore, the

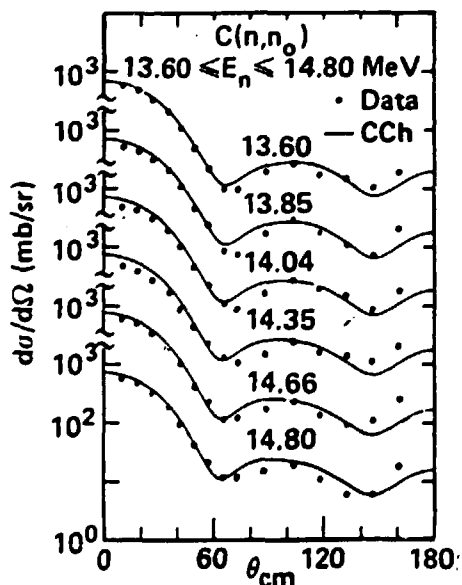


Figure 2

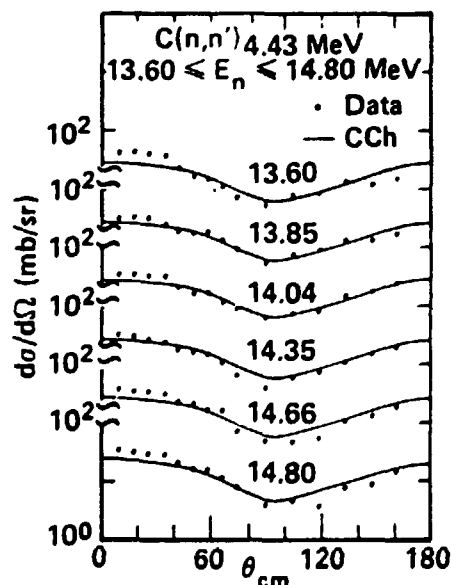


Figure 3

measurements<sup>1</sup> at 14.60 MeV are in very good agreement with the present one at 14.66 MeV. The CC calculations include the GS (0<sup>+</sup>), the 4.43 (2<sup>+</sup>) and 14.08 (4<sup>+</sup>) excited levels. Starting from the Meigooni et al.<sup>3</sup> OMP a fine tuning of the parameters was necessary to obtain the fits shown in Figs. 1-3. The initial and

final values of the parameters for set A and B are shown in Table 1. The quality of the fits to the 4.43 MeV angular distributions was most sensitive to the strength of the spin-orbit potential which is not deformed in the calculations. The fits are greatly improved by reducing the potential depth,  $V_{SO}$ , and increasing the diffuseness parameter,  $a_{SO}$ . The values of 5.50 MeV and 0.750, respectively, are in good agreement with those found from fits to neutron elastic and polarization data between 5-14 MeV.

Table 1. Values of the OMP parameters.

	$V_R$	$r_R$	$a_R$	$W_V$	$W_D$	$r_D$	$a_D$	$V_{so}$	$r_{so}$	$a_{so}$
Set A	50.78-.34E	1.22	.478+.004E	0	.45E-1.7	1.25	.27	6.20	1.05	.55
Set B	52.45-.34E	1.22	.400	0	.44E-2.2	1.25	.35	5.50	1.15	.75
	$\beta_2 = -0.53(A), -0.61(B); \beta_4 = 0.2(A \& B)$									

$^{181}\text{Ta}(n,n)$ . The CC calculation shown in Fig. 1 for the neutron elastic scattering at 14.6 MeV includes in addition to the GS ( $7/2+$ ), the 0.136 ( $9/2+$ ) and 0.301 ( $11/2+$ ) excited levels. The OMP<sup>2</sup> is the same used in the spherical OM calculations (dashed line), corrected for coupling. The value of  $\beta_2$  is 0.260. The solid curve corresponds to the sum of the angular distributions calculated for the three levels, since the resolution of the measurements ( $\approx 300$  keV) did not resolve them. No parameter search was carried out for this calculation because the levels were unresolved. The quality of the fit was greatly improved by the inclusion of coupling among the GS and excited rotational levels.

$^{232}\text{Th}, ^{238}\text{U}, ^{239}\text{Pu}(n,n)$ . For  $^{232}\text{Th}$  and  $^{238}\text{U}$

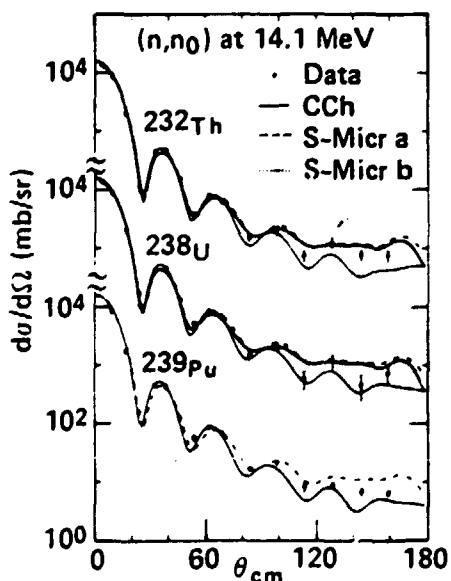


Figure 4

the CC calculations, both with phenomenological and microscopic OMP, include the  $0+$ ,  $2+$ ,  $4+$ , and  $6+$  states of the GS rotational band. For  $^{239}\text{Pu}$ , levels of the GS ( $K=1/2$ ) band are included up to the  $9/2+$  state. In Fig. 4 the measurements are compared with calculations carried out with the deformed potential of Ref. 4 (solid lines) and with two semi-microscopic calculations<sup>8</sup> to be discussed. The plotted curves correspond to the sum of the GS and excited levels differential cross-sections up to  $E_{ex} \leq 300$  keV. As for Ta, no search of parameters was carried out to optimized the fits to the data. In the semi-microscopic calculation of Lagrange et al.<sup>8</sup>, the OMP is calculated by

folding the JLM effective interaction with the deformed GS nuclear density. The differential cross sections are calculated using CC

formalism and the adiabatic rotational model. The semi-microscopic potentials have been expanded in terms of Legendre polynomials up to  $l_{\max} = 8$ , and complex coupling is used. The spin orbit potential is real and spherical. The calculations (a) and (b) (dashed and dotted lines respectively), differ in the calculation of the nuclear density. In (a),  $\rho(r)$  is obtained from a Hartree-Fock-Bogolyubov and RPA calculation; while in (b) the nucleon density distribution has been obtained from fitting electron scattering data. (For details of these calculations and respective formalism see Ref. 8). The only free parameters in the two calculations are: the ranges of the real and imaginary parts of the effective interaction,  $t_R = 1.2$  fm, and  $t_I = 1.3$  fm; the normalization factors,  $N_R = 0.94$  and  $N_I = 0.82$ , for ~~the~~ *the real and imaginary* ~~parts~~; and the strength of the spin-orbit potential,  $V_{SO} = 45$  MeV-fm<sup>5</sup>. The difference between the two calculations is small, with (b) giving slightly better results at backward angles. Both, phenomenological and semi-microscopic calculations do poorly at larger angles, and possibly could be improved by a better representation of the spin-orbit potential.

### CONCLUSIONS

This work shows conclusively the need for deformed OMP and CC formalism when calculating neutron scattering from strongly deformed nuclei. The calculations reproduce fairly well the measurements, even for nuclei as light as <sup>9</sup>Be. The fits to the C inelastic angular distributions (4.43 MeV level) need improvement. Possible effects of coupling of this level to other members of the GS rotational band or to some of the nearby vibrational levels need to be studied. The semi-microscopic calculations with effectively no free parameters (the values for  $t_R$  and  $t_I$  were obtained from <sup>208</sup>Pb data, while the magnitudes of  $N_R$ ,  $N_I$ , and  $V_{SO}$  were obtained from <sup>238</sup>U(n,n) at lower energies) give fits to the data of similar quality to those found with global OMP optimized for the actinide region. Neutron polarization data would allow a better representation of the spin-orbit potential, to which the differential cross sections at large angles are sensitive.

### REFERENCES

1. L. F. Hansen et al., UCRL 80316 Aug. 1984 (Submitted to Phys. Rev. C). L. F. Hansen et al. BAPS 29 (1984).
2. J. Rapaport et al., Nucl. Phys. A330, 15 (1979).
3. A. S. Meigooni et al., Phys. Med. Biol. 29, 643 (1984).
4. A. B. Klepalskij et al., INDC(CCP)-1511L March 1981.
5. L. F. Hansen et al., Phys. Rev. C25, 189 (1982).
6. G. Hanuot et al., Nucl. Sci. Eng. 65, 331 (1978).
7. C. A. Pearson et al., Nucl. Phys. A191, 1 (1972).
8. Ch. Lagrange et al., J. Phys. G: Nucl. Phys. 9, 197 (1983).

\*Work performed under the auspices of the U.S. DOE by the LLNL under contract number W-7405-ENG-48.

#### DISCLAIMER

This document was prepared as an account of work sponsored by an agency of the United States Government. Neither the United States Government nor the University of California nor any of their employees, makes any warranty, express or implied, or assumes any legal liability or responsibility for the accuracy, completeness, or usefulness of any information, apparatus, product, or process disclosed, or represents that its use would not infringe privately owned rights. Reference herein to any specific commercial products, process, or service by trade name, trademark, manufacturer, or otherwise, does not necessarily constitute or imply its endorsement, recommendation, or favoring by the United States Government or the University of California. The views and opinions of authors expressed herein do not necessarily state or reflect those of the United States Government thereof, and shall not be used for advertising or product endorsement purposes.